

## Supplementary Information

### **Electrochemical Trends of a Hybrid Platinum and Metal-Nitrogen-Carbon Catalyst Library for the Oxygen Reduction Reaction**

Alvin Ly<sup>1,†</sup>, Eamonn Murphy<sup>2,†</sup>, Hanson Wang<sup>2,†</sup>, Ying Huang<sup>1</sup>, Giovanni Ferro<sup>2</sup>,  
Shengyuan Guo<sup>2</sup>, Tristan Asset<sup>3</sup>, Yuanchao Liu<sup>2</sup>, Iryna V. Zenyuk<sup>1,2</sup> and  
Plamen Atanassov<sup>1,2\*</sup>

<sup>1</sup>Department of Materials Science and Engineering, National Fuel Cell Research Center (NFCRC), University of California-Irvine, Irvine, California 92697

<sup>2</sup>Department of Chemical and Biomolecular Engineering, National Fuel Cell Research Center (NFCRC), University of California-Irvine, Irvine, California 92697

<sup>3</sup>Institute of Chemistry and Processes for Energy, Environment and Health (ICPEES), UMR 7515 CNRS-Université de Strasbourg, 25 rue Becquerel, Strasbourg Cedex 02 67087, France

<sup>†</sup>Authors contributed equally to this work

\*E-mail: plamen.atanassov@uci.edu

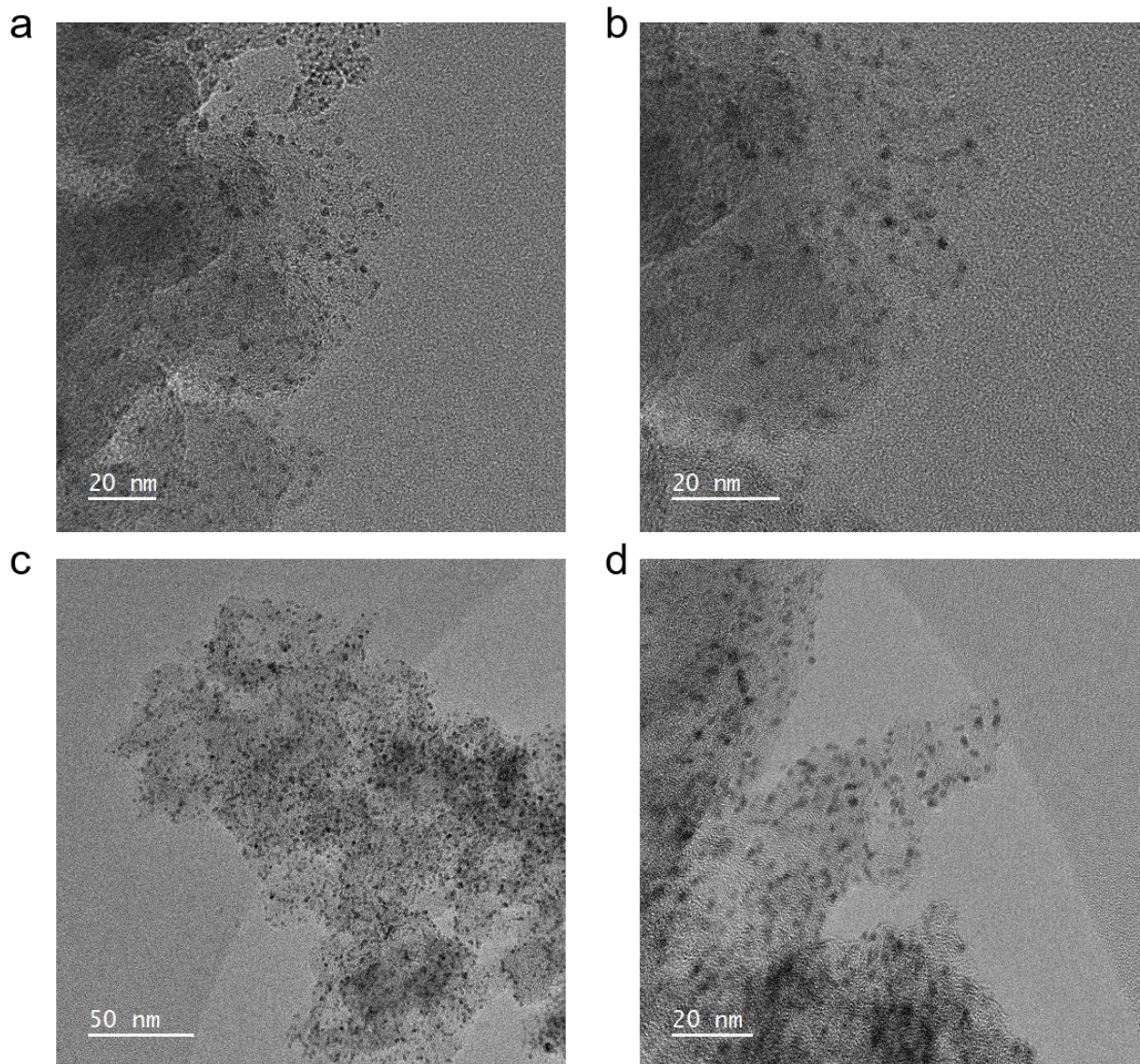


**Figure S1.** TEM images of (a & b) Pt nanoparticles on XC72R (Pt/XC72R) and (c & d) Pt nanoparticles on Ni-N-C (Pt/Ni-N-C)

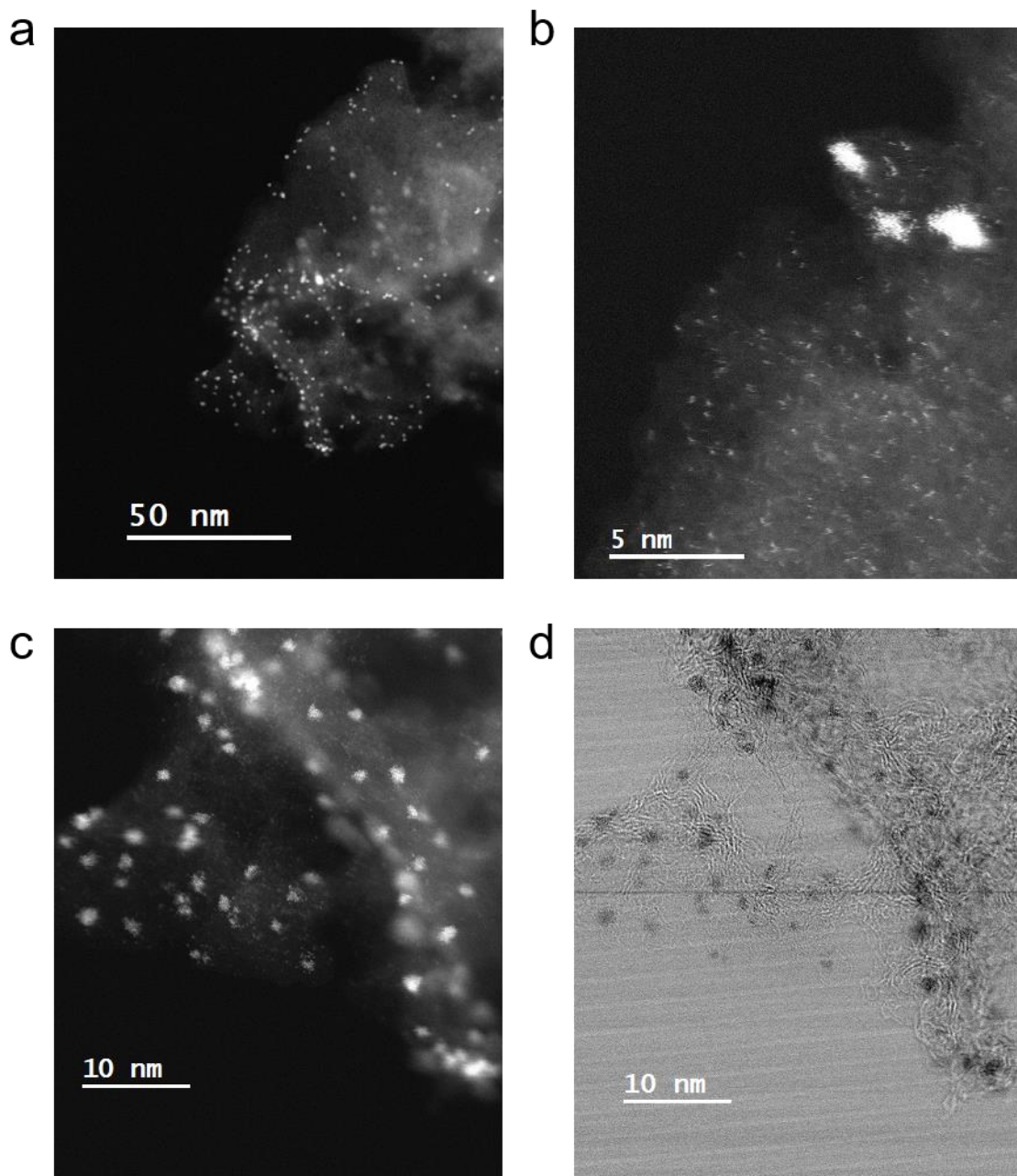


**Figure S2.** Aberration corrected STEM images of Pt on Rh-N-C (Pt/Rh-N-C) (a-c) darkfield images and (d) corresponding brightfield image of (c). The simultaneous presence of Pt nanoparticles and atomically dispersed Rh sites are observed. With the Pt nanoparticle size in general being less than 5 nm.

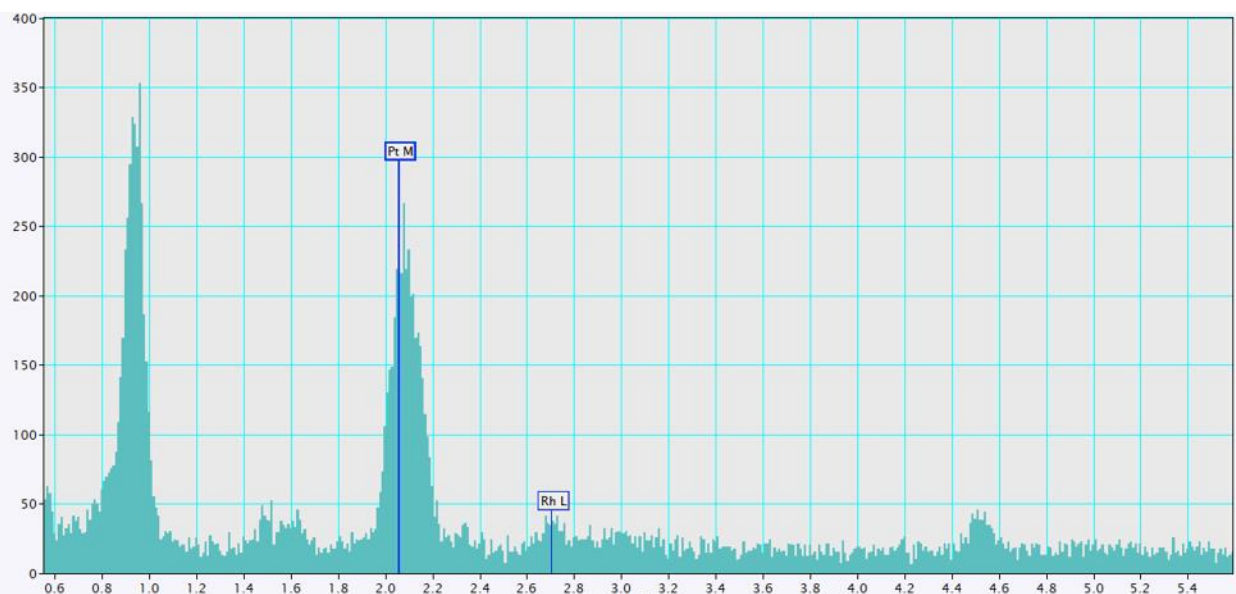
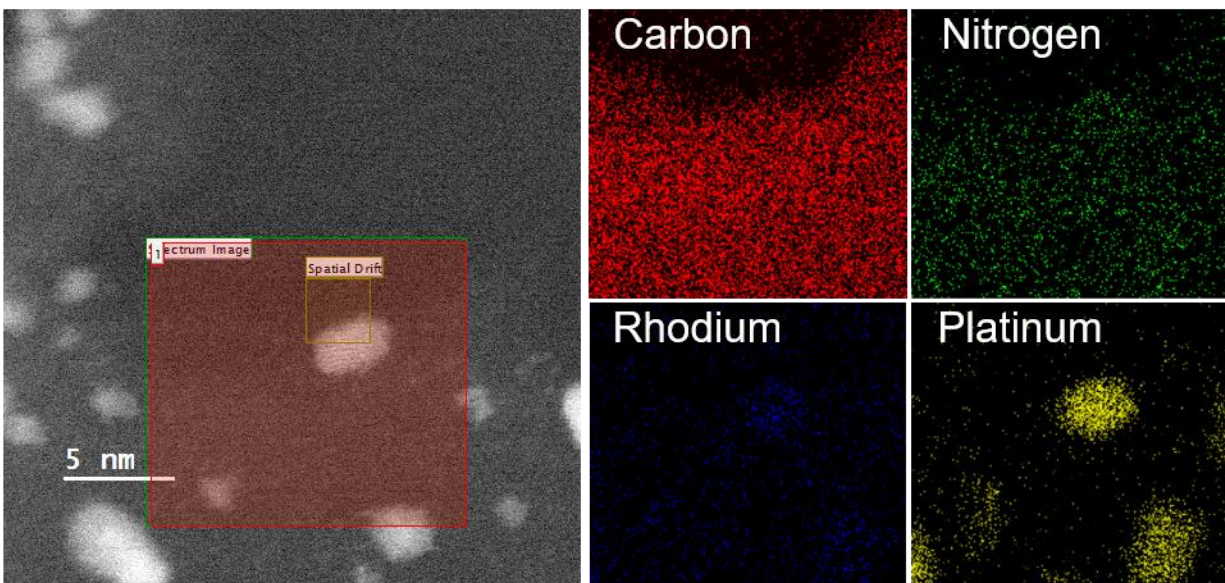


**Figure S3.** Energy dispersive X-ray spectroscopy elemental mapping of the Pt/Rh-N-C catalyst. Where Pt nanoparticles are clearly identified, with a homogenous dispersion of Rh and N from the Rh-N-C support.

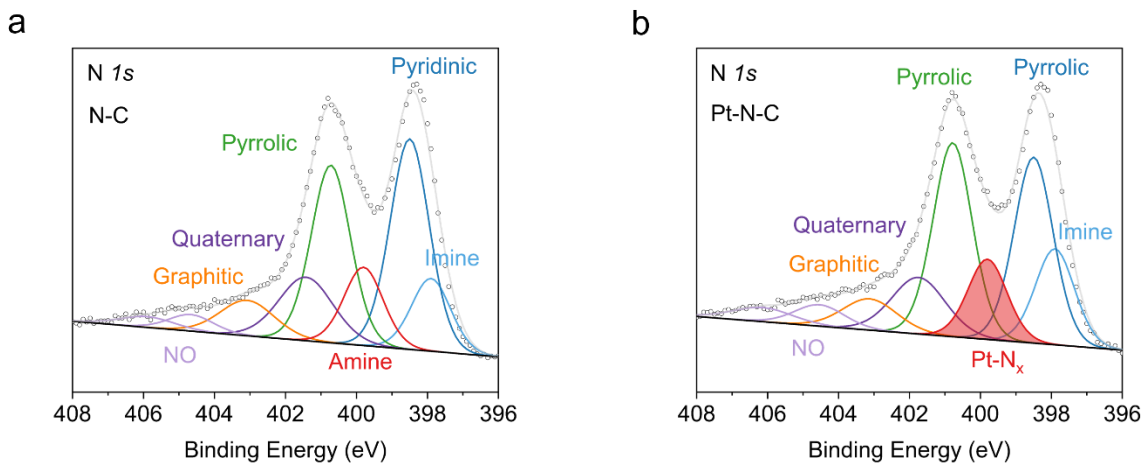


**Figure S4.** Deconvoluted high resolution N 1s XPS spectra. (a) Metal free N-C support and (b) Pt-N-C. The deconvoluted spectra shows several typical nitrogen moieties found in M-N-C materials (imine, pyridinic, amine/M-N<sub>x</sub>, pyrrolic, quaternary, graphitic and nitrogen oxides).

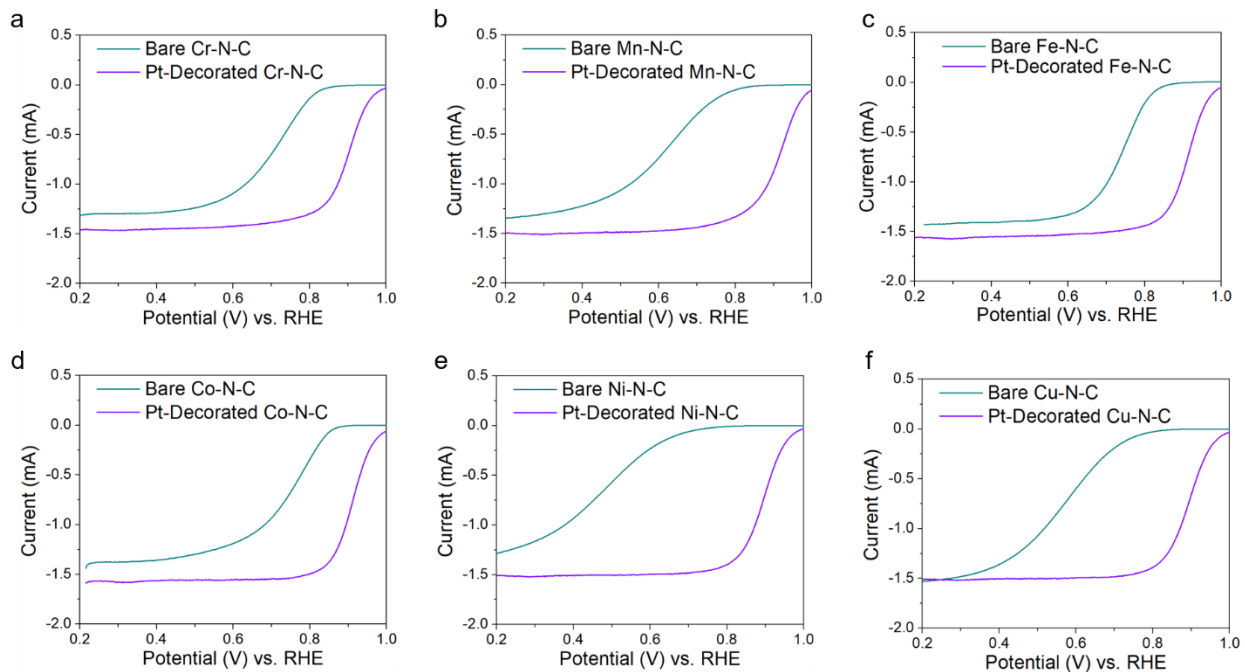


**Figure S5.** ORR performance for 3d metals evaluated by RDE in 0.1M HClO<sub>4</sub> at a scan rate of 5 mV/s. Each figure contains the LSV for the M-N-C and Pt/M-N-C materials.

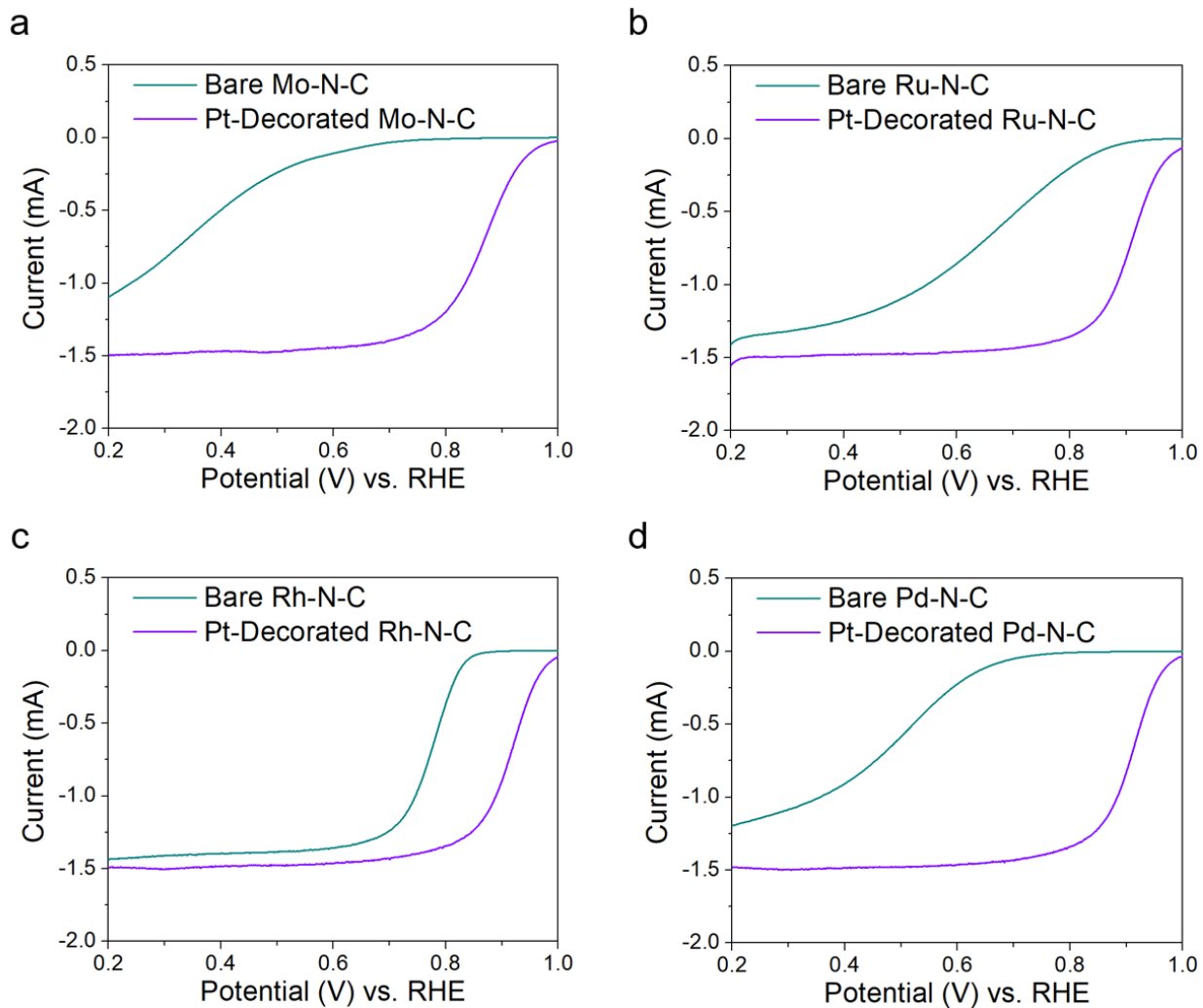


**Figure S6.** ORR performance for 4d metals evaluated by RDE in 0.1M HClO<sub>4</sub> at a scan rate of 5 mV/s. Each figure contains the LSV for the M-N-C and Pt/M-N-C materials.

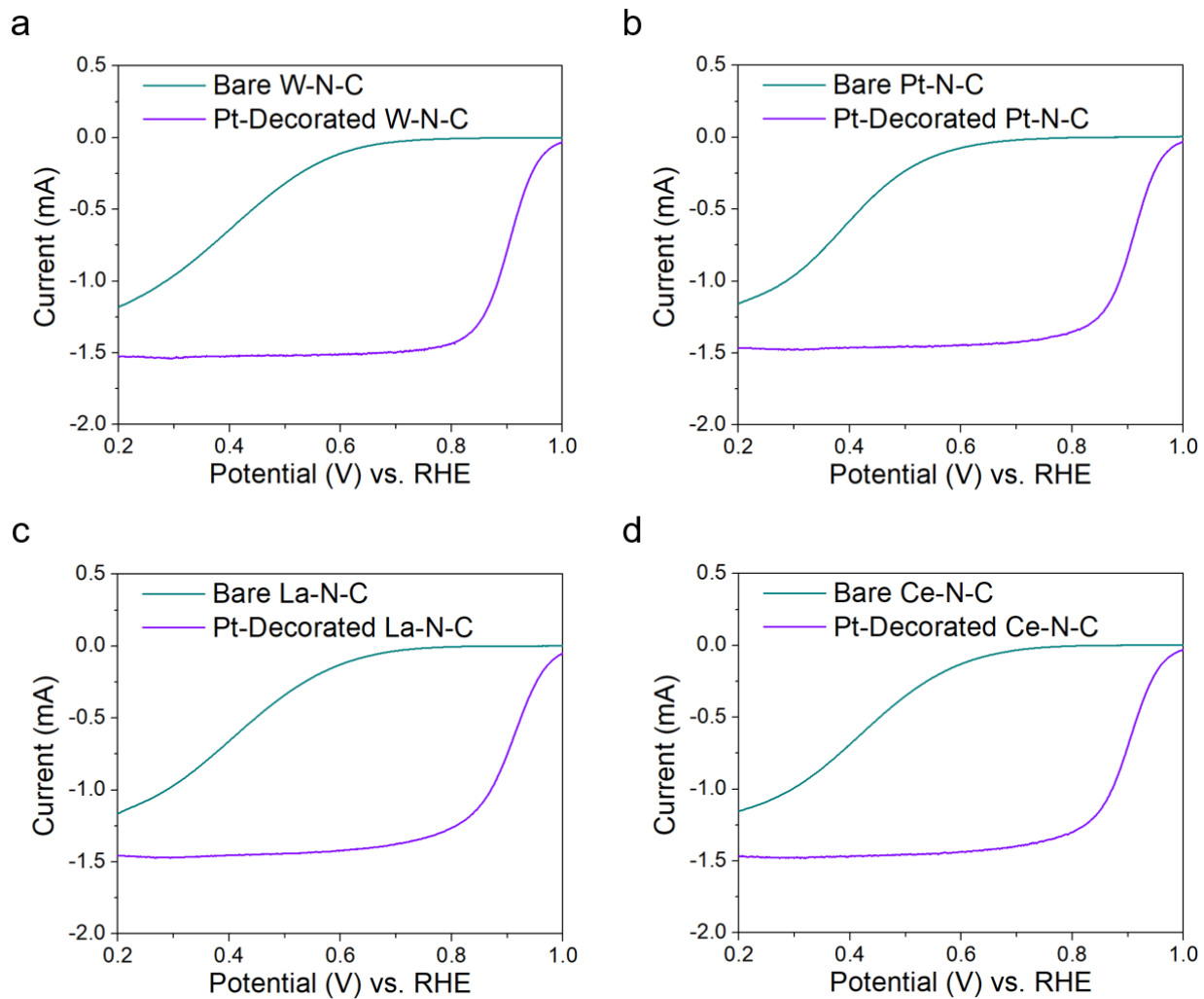


**Figure S7.** ORR performance for 5*d* and *f* metals evaluated by RDE in 0.1M HClO<sub>4</sub> at a scan rate of 5 mV/s. Each figure contains the LSV for the M-N-C and Pt/M-N-C materials.



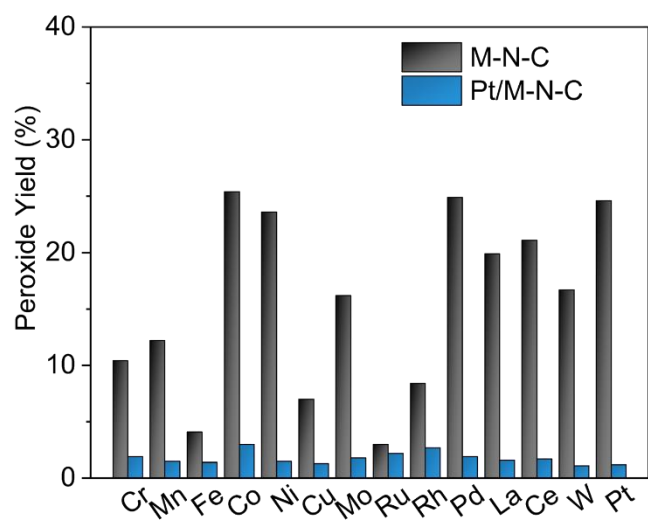


**Figure S8.** Hydrogen peroxide yields, determined from RRDE measurements in 0.1M HClO<sub>4</sub> at a scan rate of 5 mV/s.

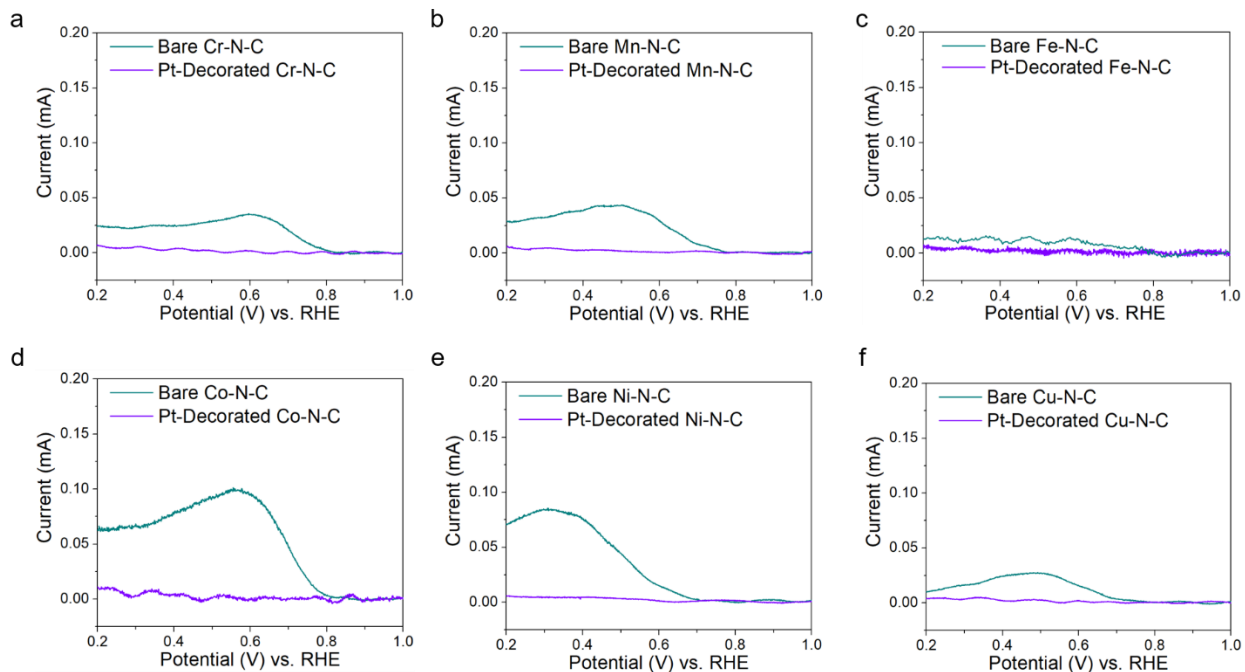


**Figure S9.** Ring currents recorded during RRDE measurements in 0.1M HClO<sub>4</sub> at a scan rate of 5 mV/s. Each figure contains the ring current for the M-N-C and Pt/M-N-C materials.

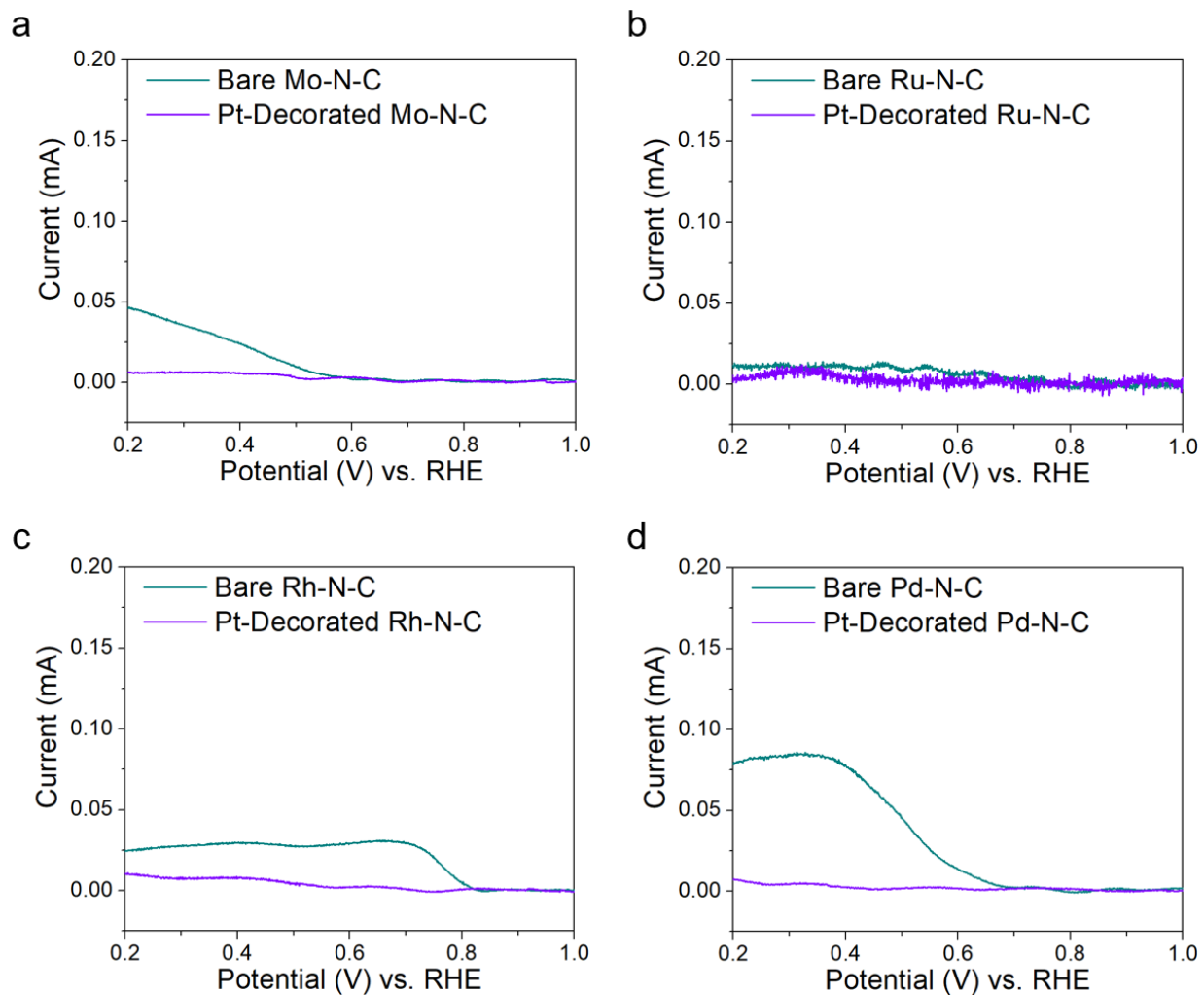


**Figure S10.** Ring currents recorded during RRDE measurements in 0.1M HClO<sub>4</sub> at a scan rate of 5 mV/s. Each figure contains the ring current for the M-N-C and Pt/M-N-C materials.

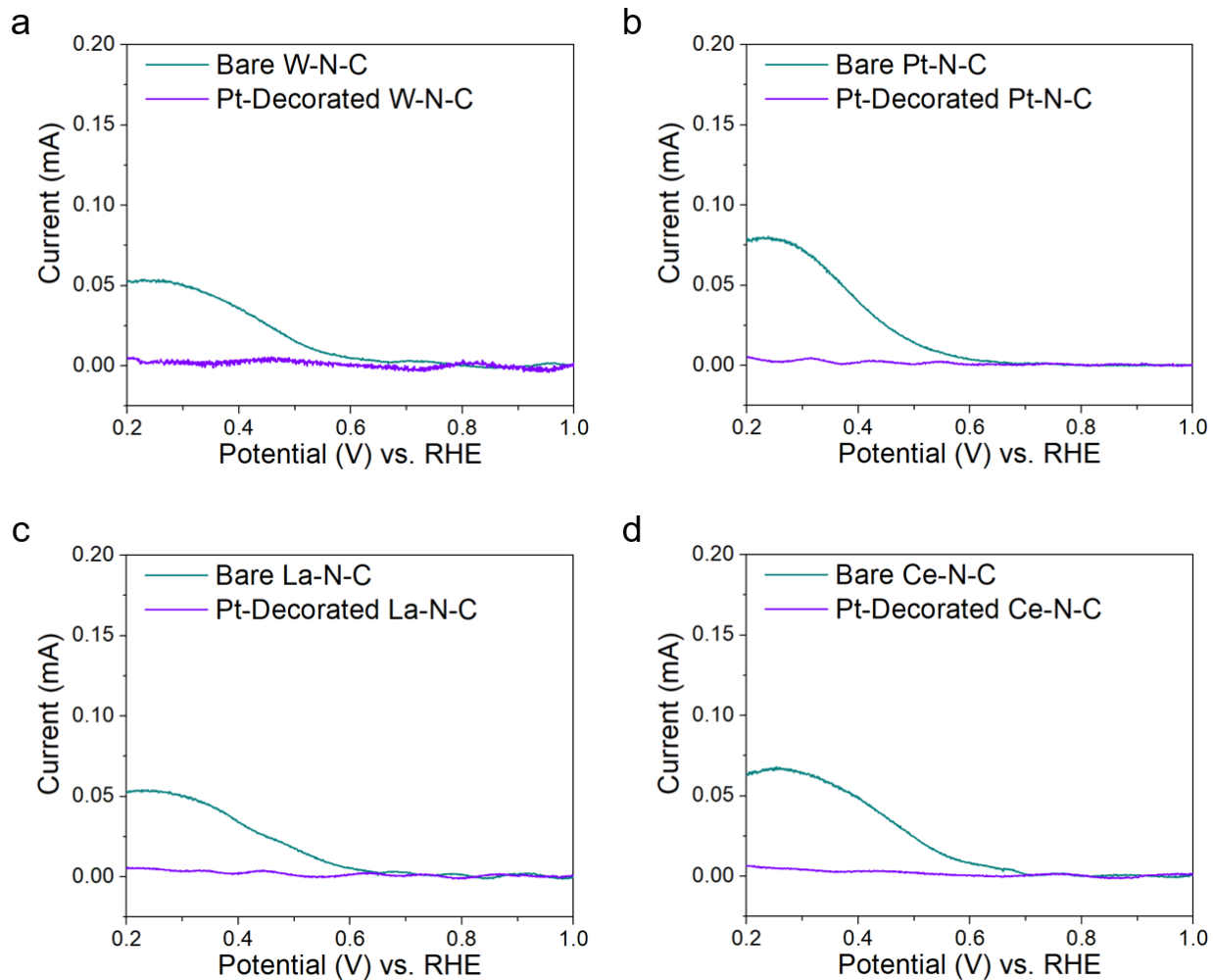


**Figure S11.** Ring currents recorded during RRDE measurements in 0.1M HClO<sub>4</sub> at a scan rate of 5 mV/s. Each figure contains the ring current for the M-N-C and Pt/M-N-C materials.

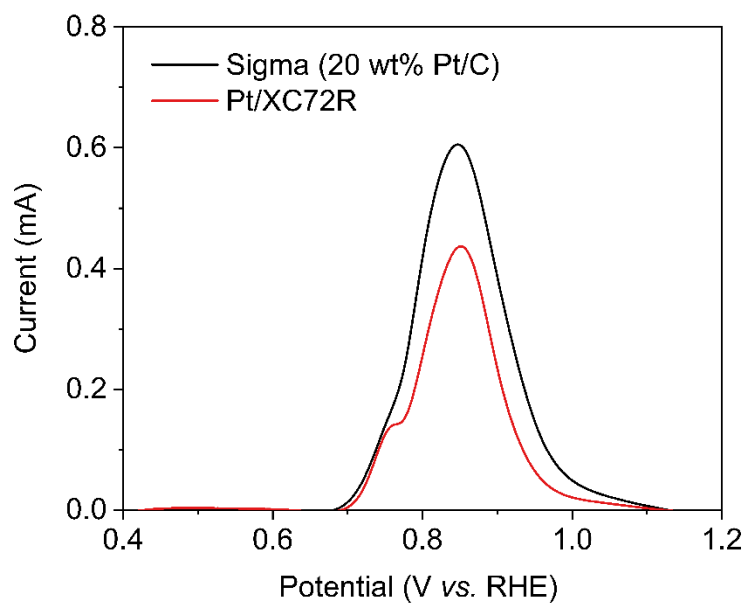


**Figure S12.** Carbon monoxide oxidation for the Pt/XC72R and Sigma (20 wt% Pt/C) reference materials. CO oxidation scans were run at 20 mV/s from 0.1 to 1.23 V vs. RHE.

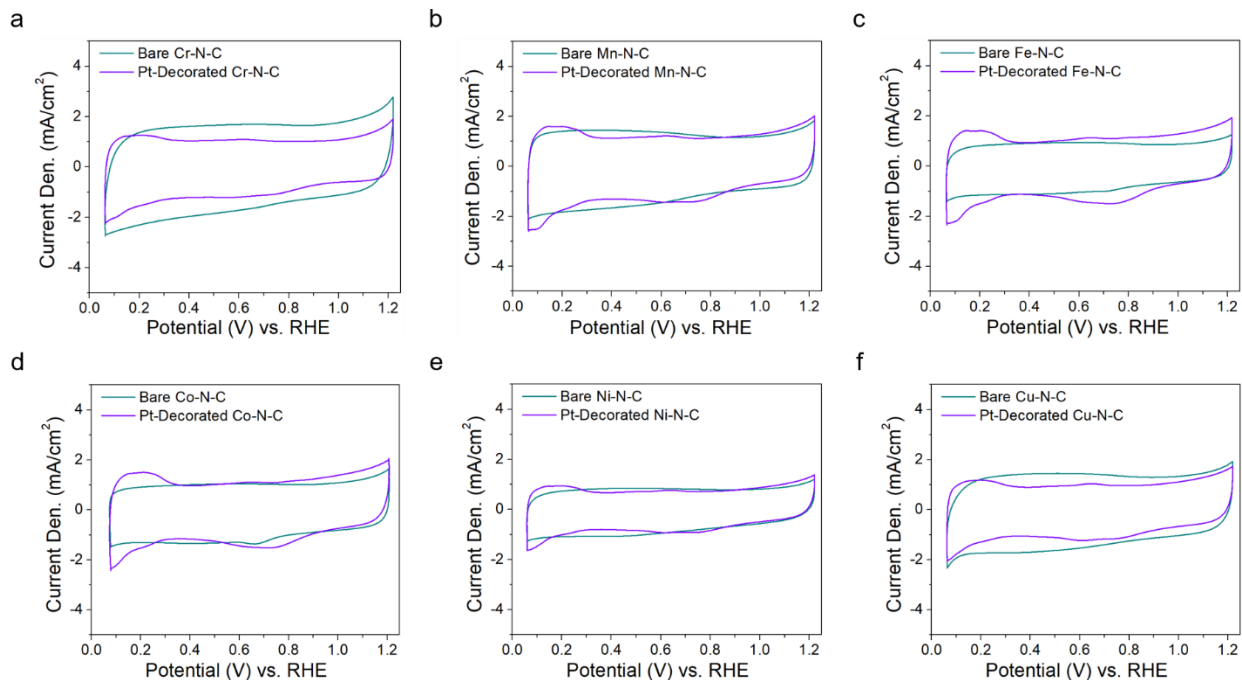


**Figure S13.** ORR CV in 0.1M HClO<sub>4</sub> recorded at a scan speed of 20 mV/s under a nitrogen atmosphere.  $H_{\text{upd}}$ -based ECSA was determined by integrating the CV between 0.05 and 0.40 V vs. RHE and calculated using Equation 1 in the main text.

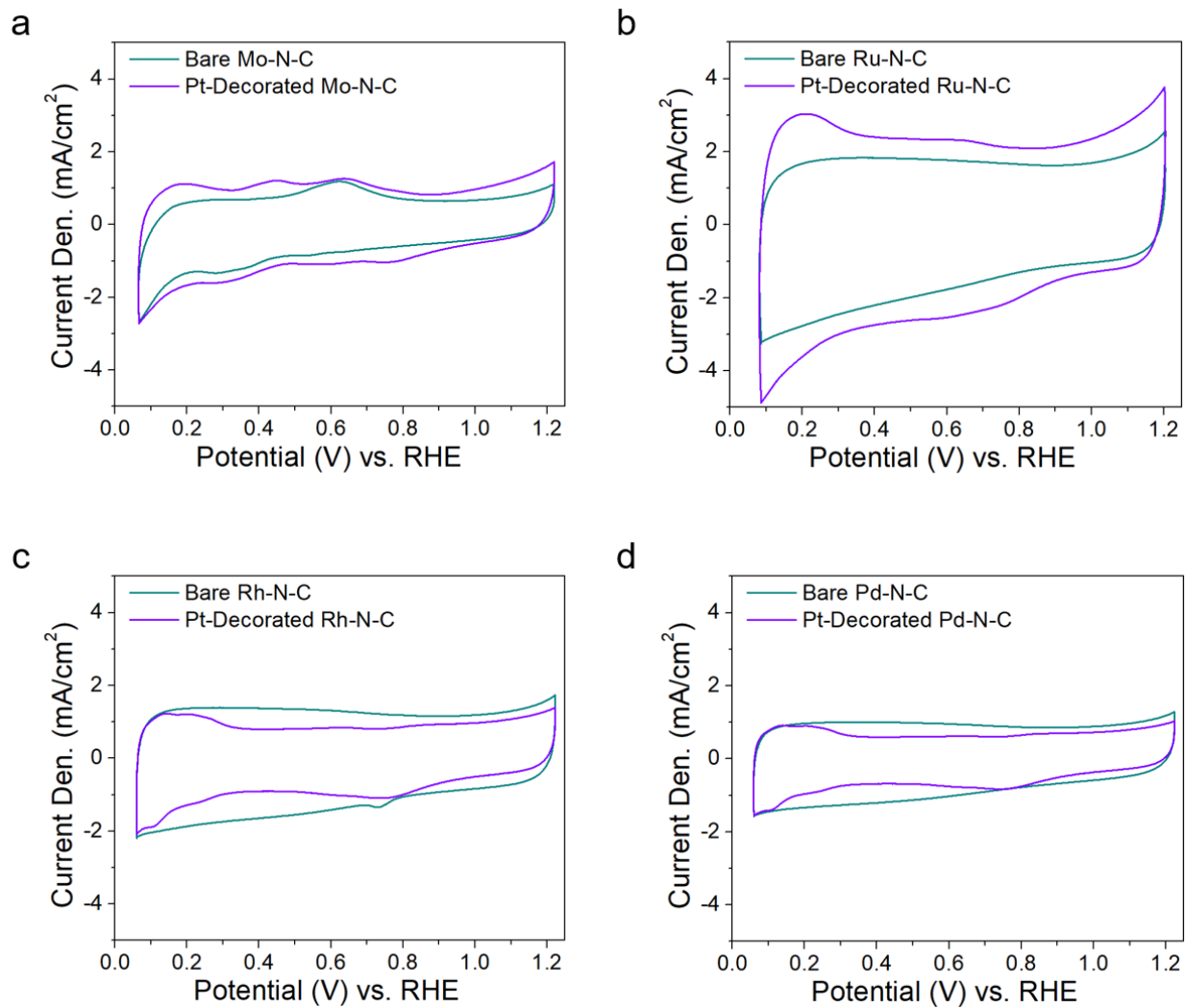


**Figure S14.** ORR CV in 0.1M HClO<sub>4</sub> recorded at a scan speed of 20 mV/s under a nitrogen atmosphere.  $H_{upd}$ -based ECSA was determined by integrating the CV between 0.05 and 0.40 V vs. RHE and calculated using Equation 1 in the main text.

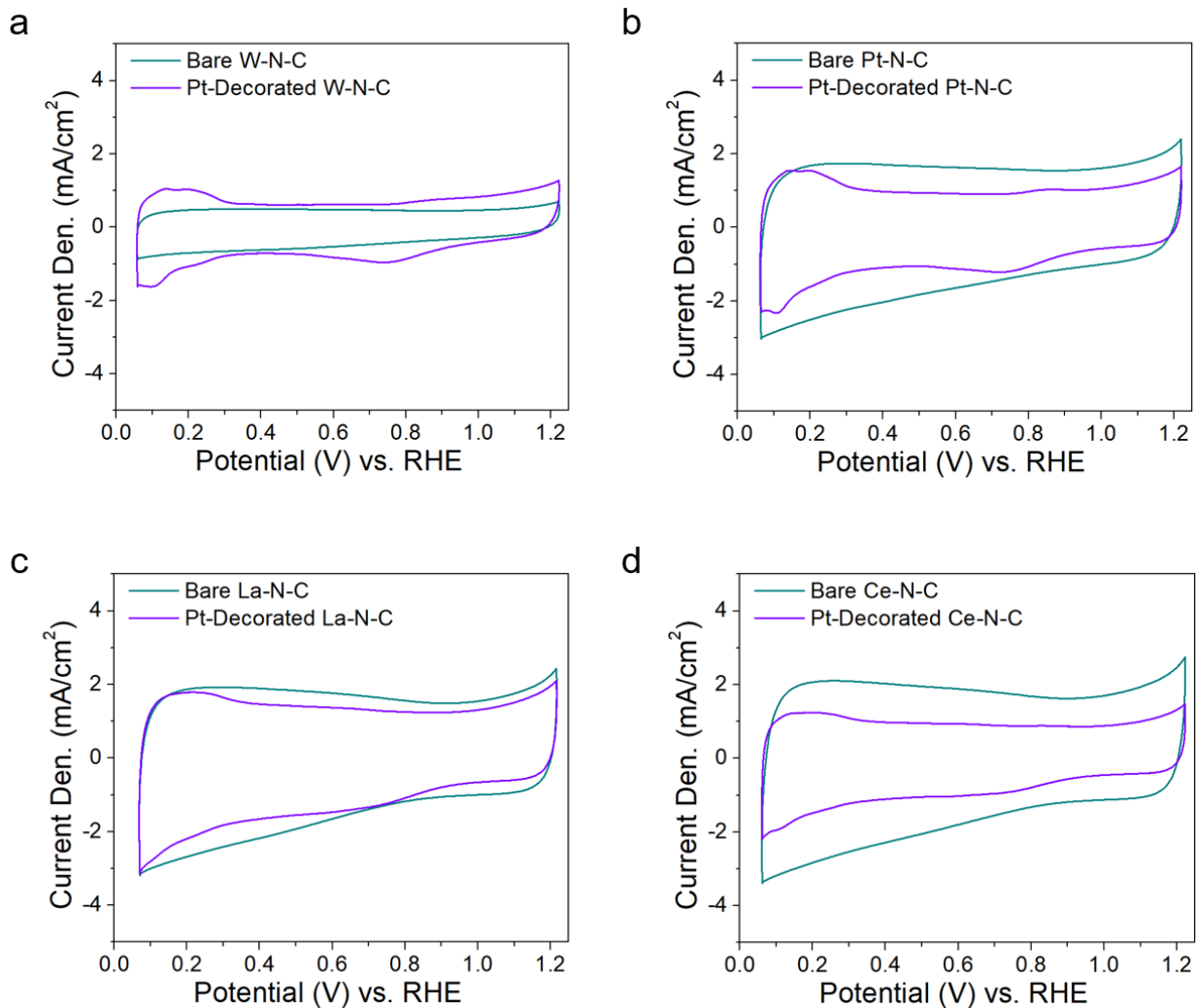


**Figure S15.** ORR CV in 0.1M HClO<sub>4</sub> recorded at a scan speed of 20 mV/s under a nitrogen atmosphere.  $H_{\text{upd}}$ -based ECSA was determined by integrating the CV between 0.05 and 0.40 V vs. RHE and calculated using Equation 1 in the main text.



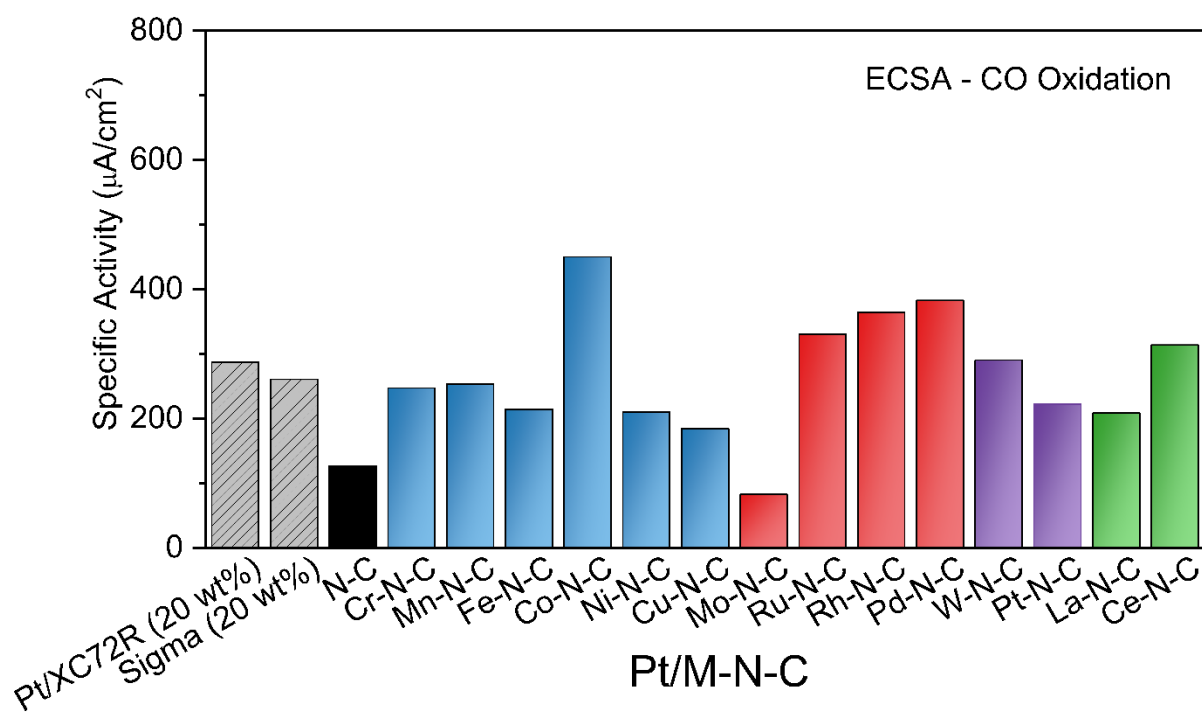


**Figure S16.** ORR specific activity for Pt/M-N-C, with the ECSA calculated from CO-oxidation.

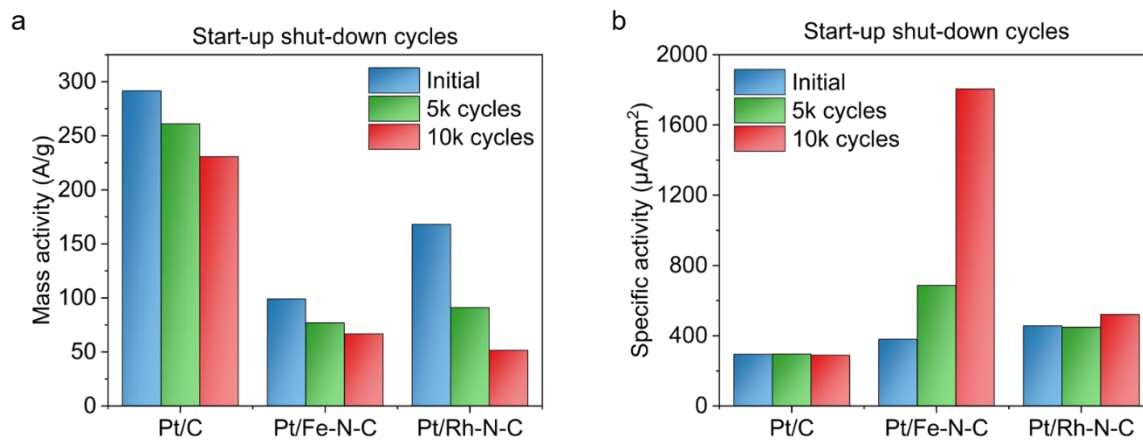


**Figure S17.** (a) Mass and (b) specific activities of the Pt/C (Sigma 20 wt%), Pt/Fe-N-C and Pt/Rh-N-C after 0, 5k and 10k cycles of the harsher, start-up shut-down cycles (1.0 – 1.5 V vs. RHE). The specific activity is calculated from the ECSA and mass activity after a given number of cycles